Scientific paper

Vanadium(V) Complexes with Bromo-Substituted Hydrazones: Synthesis, Characterization, X-ray Crystal Structures and Antimicrobial Activity

Cui-Lin Zhang,[1] Xiao-Yang Qiu[1,2,*] and Shu-Juan Liu[1]

[1] *College of Science & Technology, Ningbo University, Ningbo 315212, P.R. China*

[2] *State Key Laboratory of Structural Chemistry, Fujian Institute of Research on the Structure of Matter, Chinese Academy of Sciences, Fuzhou, Fujian 350002, P.R. China*

** Corresponding author: E-mail: xiaoyang_qiu@126.com*

Received: 05-05-2019

Abstract

Two new V^V complexes with the bromo-substituted hydrazones *N*'-(3-bromo-2-hydroxybenzylidene)-3-hydroxy-4-methoxybenzohydrazide (H_2L^1), *N*'-(3-bromo-2-hydroxybenzylidene)-3,5-dimethoxybenzohydrazide (H_2L^2), [$VOL^1(OCH_3)(CH_3OH)$] (**1**) and [$VOL^2(OCH_3)(CH_3OH)$] (**2**), were synthesized and structurally characterized by IR, UV-Vis and ^1H NMR spectroscopy, as well as single-crystal X-ray determination. The V atom in the mononuclear complexes are six-coordinated in octahedral geometry. The free hydrazones and the complexes were studied on their antibacterial activity on *S. aureus*, *B. subtilis*, *E. coli* and *P. fluorescence*, and antifungal activity on *C. albicans* and *A. niger*. The bromo groups of the hydrazone ligands may increase their antibacterial activity.

Keywords: Vanadium complex; hydrazone; crystal structure; mononuclear complex; antimicrobial activity

1. Introduction

Hydrazones and their complexes have received much interest because of their excellent biological applications in antibacterial,[1] antifungal,[2] as well as antitumor.[3] The compounds with electron-withdrawing groups have been proved to possess increased antimicrobial activity.[4] Recently, a series of chloro, fluoro, iodo- and bromo-substituted compounds have been assayed for their remarkable antimicrobial activity.[5] Schiff base vanadium complexes have distinguish antibacterial activity.[6] In pursuit of new antimicrobial material, we report herein two new bromo-substituted hydrazone compounds *N*'-(3-bromo-2-hydroxybenzylidene)-3-hydroxy-4-methoxybenzohydrazide (H_2L^1), *N*'-(3-bromo-2-hydroxybenzylidene)-3,5-dimethoxybenzohydrazide (H_2L^2), and their vanadium(V) complexes, [$VOL^1(OCH_3)(CH_3OH)$] (**1**) and [$VOL^2(OCH_3)(CH_3OH)$] (**2**), and studied their antimicrobial activities.

2. Experimental

2. 1. Materials and Methods

3-Bromosalicylaldehyde, 3-hydroxy-4-methoxybenzohydrazide, 3,5-dimethoxybenzohydrazide and VO(acac)$_2$ were obtained from Sigma-Aldrich. The remaining reagents with AR grade were obtained from Xiya Chemi-

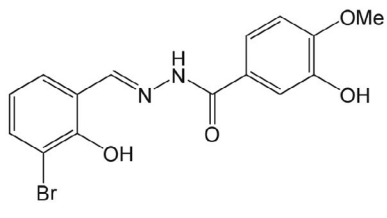

H_2L^1

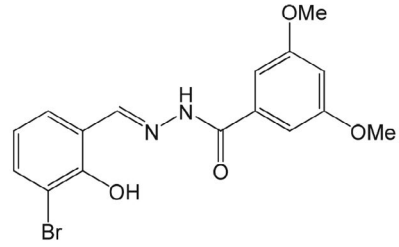

H_2L^2

cal Reagent Co. Ltd. The hydrazones were prepared by the literature method.[7] Elemental analyses (C, H, N) were determined with a Perkin-Elmer automated model 2400 Series II CHNS/O analyzer. The molar conductivity was determined using a DDS-11A conductor device. FT-IR spectra were carried out on a Perkin-Elmer 377 FT-IR spectrometer with KBr disks. The electronic spectra were performed on a Lambda 35 spectrometer. ^{1}H NMR were carried out on a Bruker 300 MHz instrument. Single crystal X-ray determination was collected on a Bruker APEX II CCD diffractometer.

2. 2. Synthesis of the Hydrazones

To the MeOH solution (30 mL) of 3-bromosalicylaldehyde (0.01 mol, 2.01 g) a MeOH solution (20 mL) of 3-hydroxy-4-methoxybenzohydrazide (0.01 mol, 1.82 g) or 3,5-dimethoxybenzohydrazide (0.01 mol, 1.96 g) was added drop wise. The solution was stirred at room temperature for 30 min, and filtered. The filtrate was evaporated to give colorless crystalline product, which were re-crystallized from MeOH and dried at reduced pressure above anhydrous $CaCl_2$.

For H_2L^1: Yield 94%. *Anal.* Calc. for $C_{15}H_{13}BrN_2O_4$: C, 49.3; H, 3.6; N, 7.7. Found: C, 49.5; H, 3.7; N, 7.6%. IR data (cm^{-1}): 3429, 3195, 1642, 1612. UV-Vis data (MeOH, λ_{max}, nm): 225, 293, 307, 325, 400. ^{1}H NMR (300 MHz, d^6-DMSO): δ 12.76 (s, 1H, O*H*), 12.30 (s, 1H, O*H*), 11.27 (s, 1H, N*H*), 8.63 (s, 1H, C*H*=N), 7.63 (d, 1H, Ar*H*), 7.50-7.40 (m, 3*H*, ArH), 7.13 (d, 1H, Ar*H*), 6.92 (t, 1H, Ar*H*), 3.85 (s, 3H, OCH_3). For H_2L^2: Yield 97%. *Anal.* Calc. for $C_{16}H_{15}BrN_2O_4$: C, 50.68; H, 3.99; N, 7.39. Found: C, 50.53; H, 4.08; N, 7.46%. IR data (cm^{-1}): 3433, 3197, 1644, 1612. UV-Vis data (MeOH, λ_{max}, nm): 225, 295, 307, 328, 400. ^{1}H NMR (300 MHz, d^6-DMSO): δ 12.65 (s, 1H, O*H*), 11.33 (s, 1H, N*H*), 8.63 (s, 1H, C*H*=N), 7.63 (d, 1H, Ar*H*), 7.45 (d, 1*H*, ArH), 6.92 (t, 1H, Ar*H*), 6.71 (s, 1H, Ar*H*), 6.45 (d, 2H, Ar*H*), 3.84 (s, 6H, OCH_3).

2. 3. Synthesis of the Complexes

The MeOH solution (10 mL) of hydrazones (0.10 mmol each) was reacted with the MeOH solution (10 mL) of VO(acac)$_2$ (0.10 mmol, 26.5 mg). The solution was stirred and refluxed for 1 h, and cooled to room temperature. Brown single crystals were generated upon slowly evaporation within 6 days. The crystals were washed with MeOH and dried at reduced pressure above anhydrous $CaCl_2$.

For **1**: Yield 36%. Anal. calc. for $C_{17}H_{18}BrN_2O_7V$: C, 41.4; H, 3.7; N, 5.7; found: C, 41.3; H, 3.7; N, 5.6%. IR data (cm^{-1}): 3454 (w), 1603 (s), 958 (m). UV-Vis data (MeOH, λ_{max}, nm): 272, 335. ^{1}H NMR (300 MHz, d^6-DMSO): δ 12.71 (s, 1H, O*H*), 12.20 (s, 1H, O*H*), 9.39 (s, 1H, Ar*H*), 8.56 (s, 1H, C*H*=N), 7.61 (q, 1H, Ar*H*), 7.51-7.41 (m, 2H, Ar*H*), 7.08 (d, 1H, Ar*H*), 6.91 (t, 1H, Ar*H*), 3.86 (s, 3H, OCH_3), 3.33 (s, 6H, CH_3OH and OCH_3). Λ_M (10^{-3} M in

Table 1. Crystallographic and refinement data for complexes **1** and **2**

Complex	H_2L^1	1	2
Formula	$C_{15}H_{13}BrN_2O_4$	$C_{17}H_{18}BrN_2O_7V$	$C_{18}H_{20}BrN_2O_7V$
Formula weight	365.18	493.18	507.21
T (K)	298(2)	298(2)	298(2)
Crystal system	Monoclinic	Triclinic	Monoclinic
Space group	$P2_1/c$	P–1	$P2_1/n$
a (Å)	17.2603(13)	7.6101(9)	13.5326(10)
b (Å)	7.2902(12)	10.3404(13)	9.3050(7)
c (Å)	12.1706(19)	13.1269(16)	16.1808(13)
α (°)	90	81.517(1)	90
β (°)	104.431(1)	75.965(1)	94.621(1)
γ (°)	90	68.939(1)	90
V (Å^3)	1483.1(4)	933.1(2)	2030.9(3)
Z	4	2	4
D_{calc} (g cm^{-3})	1.635	1.755	1.659
μ (Mo Kα) (mm^{-1})	2.791	2.716	2.499
F(000)	736	496	1024
Measured reflections	8532	8761	18003
Unique reflections	2764	3455	3606
Observed reflections ($I \geq 2s(I)$)	1896	2906	2900
Parameters	205	260	269
Restraints	1	1	1
Goodness of fit on F^2	1.025	1.030	1.039
R_1, wR_2 [$I \geq 2\sigma(I)$][a]	0.0437, 0.1036	0.0285, 0.0679	0.0345, 0.0776
R_1, wR_2 (all data)[a]	0.0717, 0.1159	0.0378, 0.0721	0.0498, 0.0857

[a] $R_1 = F_o - F_c/F_o$, $wR_2 = [\sum w(F_o^2 - Fc^2)/\sum w(F_o^2)^2]^{1/2}$

acetonitrile): 41 Ω^{-1} cm^2 mol^{-1}. For **2**: Yield 41%. Anal. calc. for $C_{18}H_{20}BrN_2O_7V$: C, 42.62; H, 3.97; N, 5.52; found: C, 42.73; H, 3.89; N, 5.61%. IR data (cm^{-1}): 3450 (w), 1602 (s), 953 (m). UV-Vis data (MeOH, λ_{max}, nm): 275, 323. ^{1}H NMR (300 MHz, *d*^{6}-DMSO): δ 12.56 (s, 1H, O*H*), 9.30 (s, 1H, Ar*H*), 8.59 (s, 1H, C*H*=N), 7.66 (d, 1H, Ar*H*), 7.53 (d, 1H, Ar*H*), 7.17-6.91 (m, 2H, Ar*H*), 6.70 (s, 1H, Ar*H*), 3.84 (s, 3H, OCH_3), 3.78 (s, 3H, OCH_3), 3.38 (s, 6H, CH_3OH and OCH_3). Λ_M (10^{-3} M in acetonitrile): 32 Ω^{-1} cm^2 mol^{-1}.

2. 4. X-ray Crystallography

Single crystal X-ray determination was performed on a Bruker APEX II CCD area diffractometer with Mo Kα radiation at 0.71073 Å. The data were reduced with the program SAINT,[8] and corrected by multi-scan using the program SADABS.[9] The vanadium complexes were solved readily by direct method. The complexes were refined by the full-matrix least-squares method against F^2 using the program SHELXTL.[10] The non-H atoms were anisotropically refined. The H atoms of the methanol molecules were assigned from the difference Fourier maps, and isotropically refined with $d_{O\text{-}H}$ restrained to 0.85(1) Å. The other H atoms were in calculated geometrical positions. The crystallographic data and refinement parameters are summarized in Table 1.

2. 5. Antimicrobial Study

The activities against *B. subtilis*, *S. aureus*, *E. coli*, and *P. fluorescence* of the compounds were assayed with MH (Mueller–Hinton) medium. The activities against *C. albicans* and *A. niger* of the compounds were assayed with RPMI-1640 medium. The dye MTT was used in the determination of the MIC values by a colorimetric method.[11] A specified quantity of the medium with the tested compound was poured into micro-titration plates. Suspension of the microorganism containing 1.0×10^5 cfu mL^{-1} was applied to micro-titration plates with the compounds in DMSO to be tested and incubated at 37 °C for 24 h and 48 h for bacteria and fungi, respectively. The MIC values were visually determined on each of the microtitration plates, Phosphate buffered saline (50 μL, 0.01 mol L^{-1}, pH = 7.4) containing 2 mg of MTT · mL^{-1} was poured into the well. Incubation was continued for 4–5 h at room temperature. The content of the well was removed and isopropanol (100 μL) containing 5% 1 mol L^{-1} HCl was added to extract the dye. The optical density was determied with a micro-plate reader at 550 nm after 12 h of incubation at room temperature.

3. Results and Discussion

3. 1. Chemistry

The hydrazones H_2L^1 and H_2L^2 were synthesized by the reaction of 3-bromosalicylaldehyde and 3-hydroxy-4-methoxybenzohydrazide and 3,5-dimethoxybenzohydrazide, respectively in ethanol. The vanadium complexes were synthesized by the reaction of the hydrazones H_2L^1 and H_2L^2 with $VO(acac)_2$ in MeOH followed by re-crystallization. Elemental analyses (C, H, N) of the complexes are in accordance with the results of single-crystal X-ray analysis.

3. 2. Spectroscopic Studies

In the spectra of the compounds, the broad and weak absorptions at 3400–3500 cm^{-1} can be attributed to the ν(O–H). The sharp and weak bands of H_2L located at *ca.* 3195 cm^{-1} can be attributed to the ν(N–H). The strong absorption at 1643 cm^{-1} of H_2L are generated by ν(C=O), whereas the typical bands at 1612 cm^{-1} are the ν(C=N). The absence of the ν(C=O) and ν(N–H) in the spectra of the complexes, suggests that the hydrazone ligands are enolized during the coordination. The intense bands at 1602 cm^{-1} of the complexes are due to the ν(C=N). The characteristic ν(V=O) at 955 cm^{-1} for the complexes can be obviously identified.[12]

The bands in the UV-Vis spectra of the compounds at 320–340 nm are attributed to the intra-ligand $\pi \rightarrow \pi^*$ absorption. The lowest energy transition bands of the complexes are located at 400 nm, which can be attributed to LMCT transition. The LMCT and to some extent $\pi \rightarrow \pi^*$ bands observed at 275 nm for complexes **1** and **2** are attributed to the O donor atoms bound to V atoms.[12]

The ^{1}H NMR spectra of the free hydrazones H_2L^1 and H_2L^2 exhibit OH (phenolic) resonances at 12.76 and 12.30 ppm, and 12.65 ppm, respectively. Signals for one CH proton at 8.63 ppm, and one NH proton at 11.27 ppm for H_2L^1, and signals for one CH=N proton at 8.63 ppm, and one NH proton at 11.33 ppm for H_2L^2. Signals for aromatic protons are found in the 7.63–6.45 ppm range. Signals for methoxy protons are found at about 3.84–3.85 ppm. The ^{1}H NMR spectrum of complex **1** exhibits two sets of proton signals at 12.71 and 12.20 ppm, and that of complex **2** exhibits one proton signal at 12.56 ppm. There are no NH signals observed, indicating the coordination of the hydrazones through enolate form. The aromatic protons appear in the range 9.39–6.70 ppm. In addition, there exhibits bands at 3.33–3.38 ppm due to the coordinated methoxide and methanol ligands. The CH=N proton signals are observed at 8.56 ppm for **1** and 8.59 ppm for **2**.

3. 3. Structure Description of H_2L^1

The molecular structure of H_2L^1 is depicted in Figure 1. The compound adopts *E* configuration about the CH=N unit. The methylidene bond C7–N1 (1.281(5) Å) is within typical double bond. The distance of C8–N2 bond (1.356(4) Å) is shorter, and the distance of C8–O2 bond (1.230(4) Å) is longer than usual, suggests the conjugation effects in the hydrazone molecule. The bond values are within normal ranges.[4a] The two aromatic rings form a dihedral angle of

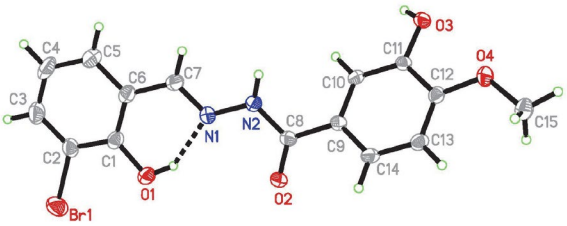

Figure 1. A perspective view of H_2L^1 with the atom labeling scheme. Thermal ellipsoids are drawn at the 30% probability level. Hydrogen bond is indicated by a dotted line.

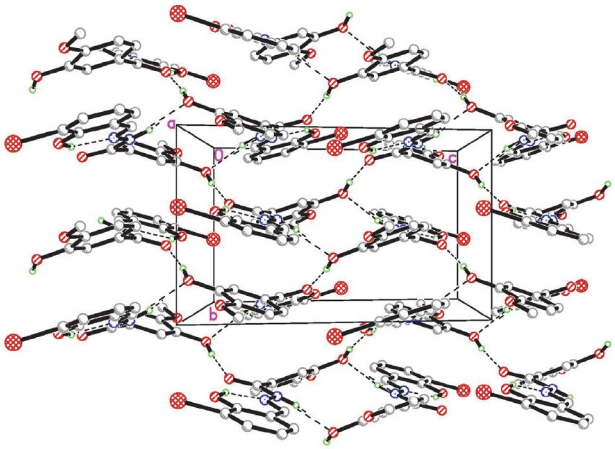

Figure 2. Molecular packing structure of H_2L^1, with hydrogen bonds indicated by dotted lines.

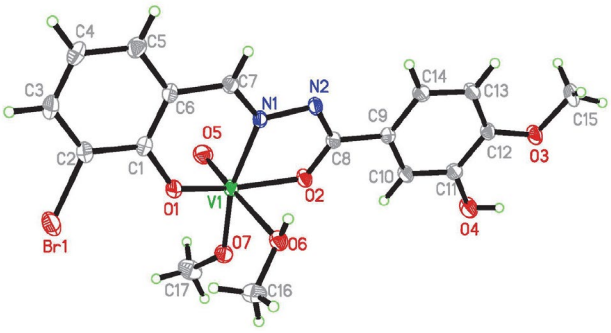

Figure 3. A perspective view of complex **1** with the atom labeling scheme. Thermal ellipsoids are drawn at the 30% probability level.

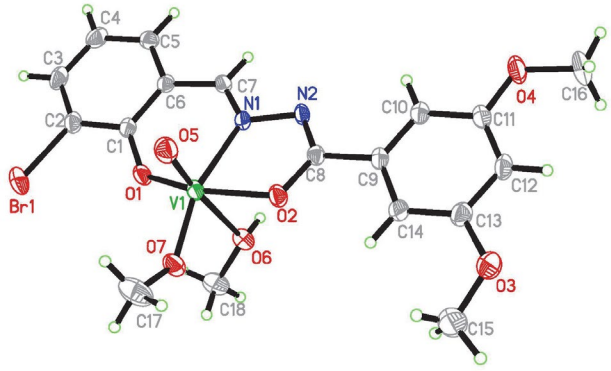

Figure 4. A perspective view of complex **2** with the atom labeling scheme. Thermal ellipsoids are drawn at the 30% probability level.

39.0(3)°. Crystal structure of the compound is stabilized by intermolecular hydrogen bonds (Table 3, Figure 2).

3. 4. Structure Description of the Vanadium Complexes

The molecular structures of the vanadium complexes are depicted in Figures 3 and 4, respectively. Selected bond lengths and angles are listed in Table 2. The V atoms are in distorted octahedral geometry with the hydrazone ligand coordinated in a meridional fashion. The hydrazones form five- and six-membered chelate rings with the V atoms. The chelate angles are 74.0–74.2° and 82.8–83.5°, respectively, which are not uncommon for this type of ligand systems.[13] The hydrazone ligand lies in a plane with one hydroxylato ligand which lies *trans* to the hydrazone imino N atom. One O atom of the MeOH ligand *trans* to the oxido group completes the octahedral geometry at rather elongated distances of 2.40–2.44 Å. The displacements of the V atoms from the planes defined by the four equatorial donors toward the apical oxido atoms are 0.32–0.33Å. The hydrazones coordinate in their doubly deprotonated enolate form which is consistent with the observed O2–C8 and N2–C8 bond lengths of about 1.29–1.32 Å. This agrees with reported metal complexes containing the enolate form of this ligand type.[14]

In the crystal structure of complex **1**, the molecules are linked by intermolecular hydrogen bonds (Table 3), leading to the formation of 3D network (Figure 5). In the crystal structure of complex **2**, the molecules are linked by hydrogen bonds (Table 3), leading to the formation of dimers (Figure 6).

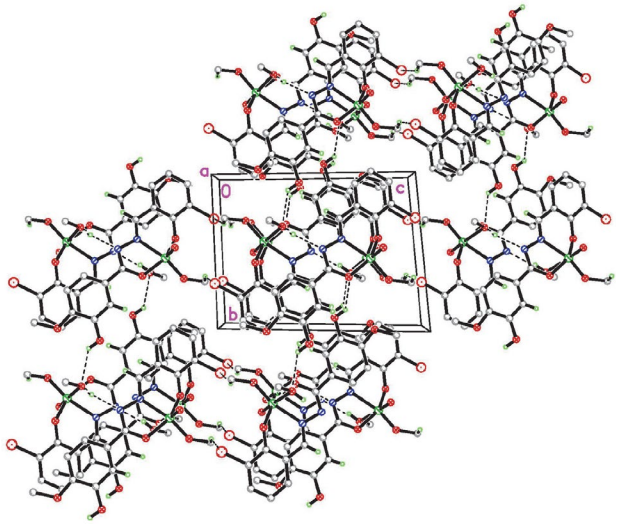

Figure 5. Crystal structure of complex **1**, with hydrogen bonds indicated by dotted lines.

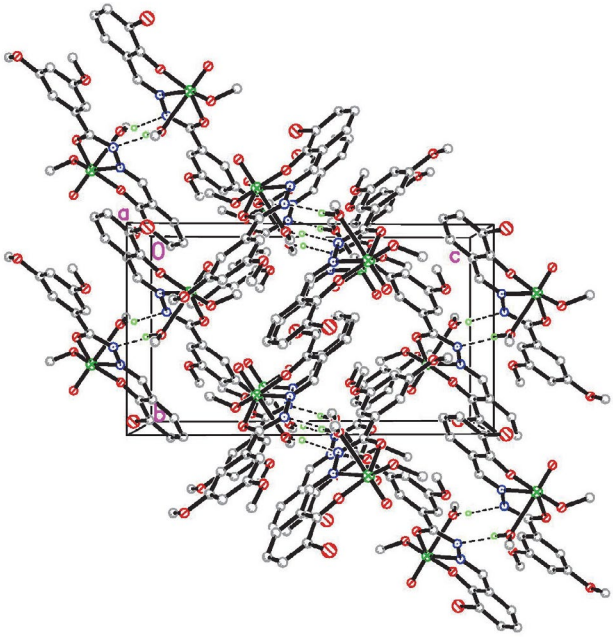

Figure 6. Crystal structure of complex **2**, with hydrogen bonds indicated by dotted lines.

Table 2. Selected bond distances (Å) and angles (°) for the complexes

	1	**2**
V1–O1	1.8676(16)	1.8594(18)
V1–O2	1.9309(15)	1.9445(18)
V1–O5	1.5831(17)	1.581(2)
V1–O6	2.4343(17)	2.407(2)
V1–O7	1.7698(16)	1.7559(19)
V1–N1	2.1330(18)	2.129(2)
O5–V1–O7	102.51(8)	103.79(11)
O5–V1–O1	99.01(9)	99.96(10)
O7–V1–O1	98.66(7)	99.68(9)
O5–V1–O2	100.53(8)	97.85(10)
O7–V1–O2	97.74(7)	96.05(9)
O1–V1–O2	151.03(7)	152.61(9)
O5–V1–N1	96.04(8)	96.01(10)
O7–V1–N1	160.86(7)	159.01(9)
O1–V1–N1	82.88(7)	83.45(8)
O2–V1–N1	74.00(6)	74.12(8)
O5–V1–O6	177.35(8)	174.54(9)
O7–V1–O6	80.15(7)	80.79(8)
O1–V1–O6	80.48(7)	82.00(8)
O2–V1–O6	79.01(6)	78.55(8)
N1–V1–O6	81.32(6)	79.10(7)

Table 3. Hydrogen bond values for the compounds

D*–H···*A	***d*(*D*–*H*)**	***d*(H···*A*)**	***d*(*D*···*A*)**	**Angle (*D*–H···*A*)**
H_2L^1				
N3–H2···O3^{i}	0.90(1)	2.00(1)	2.885(3)	169(4)
O3–H3···O2^{ii}	0.82	1.84	2.654(3)	172(4)
O1–H1···N1	0.82	1.87	2.577(4)	144(4)
1				
O4–H4···O6^{iii}	0.82	2.39	3.009(2)	133(5)
O6–H6···N2	0.84(1)	2.06(1)	2.893(2)	171(3)
C7–H7···O4^{iv}	0.93	2.58	3.381(2)	144(5)
2				
O6–H6···N2^{v}	0.85(1)	2.07(1)	2.911(3)	172(4)

Symmetry codes: (i) 1 – *x*, 1 – *y*, 1 – *z*; (ii) *x*, ½ – *y*, ½ + *z*; (iii) *x*, 1 + *y*, *z*; (iv) *x*, –1 + *y*, *z*; (v) 1 – *x*, 1 – *y*, – *z*.

3. 5. Antimicrobial Activity

The free hydrazones and the complexes were assayed for antibacterial activities against two Gram (+) bacterial strains (*B. subtilis* and *S. aureus*) and two Gram (–) bacterial strains (*E. coli* and *P. fluorescence*) by MTT method. The MIC (minimum inhibitory concentration, μg mL^{-1}) values are given in Table 4. Penicillin G was assayed as the reference drug. Both the free hydrazones show medium activity against *B. subtilis* and *S. aureus*, weak activity against *P. fluorescence*, and no activity against *E. coli*. The two vanadium(V) complexes in this work have superior activity against the bacteria than the free hydrazones. The complexes have excellent activity against *B. subtilis*, *S. aureus* and *E. coli* which are comparable to Penicillin G. Complex **1** has no activity against *P. fluoresence*, while complex **2** has weak activity. Both complexes have no activity on the fungal strains *Aspergillus niger* and *Candida albicans*.

Table 4. Antimicrobial results with MIC (μg mL^{-1})

	B. subtilis	***S. aureus***	***E. coli***	***P. fluorescence***
H_2L^1	37.5	18.8	75	> 150
H_2L^2	18.8	18.8	75	> 150
1	4.6	9.4	9.4	> 150
2	2.3	9.4	9.4	75
Penicillin G	2.3	4.7	>150	> 150

4. Supplementary Data

CCDC 1913947 (H_2L^1), 1913948 (**1**) and 1913949 (**2**) contain the supplementary crystallographic data for the compounds. The data can be obtained free of charge *via* http://www.ccdc.cam.ac.uk/conts/retrieving.html, or from the Cambridge Crystallographic Data Centre, 12

Union Road, Cambridge CB2 1EZ, UK; fax: (+44) 1223-336-033; or e-mail: deposit@ccdc.cam.ac.uk.

5. Acknowledgments

This work was financially supported by K.C. Wong Magna Fund in Ningbo University, Ningbo Natural Science Fund (Project No. 201701HJ-B01019), State Key Laboratory Development Fund of Structural Chemistry and Ningbo Education Research Project (Project No. 2017YZD001).

6. References

1. (a) K. Pyta, A. Janas, M. Szukowska, P. Pecyna, M. Jaworska, M. Gajecka, F. Bartl, P. Przybylski, *Eur. J. Med. Chem.* **2019**, *167*, 96–104;**DOI:**10.1016/j.ejmech.2019.02.009
(b) R. Fekri, M. Salehi, A. Asadi, M. Kubicki, *Inorg. Chim. Acta* **2019**, *484*, 245–254; **DOI:**10.1016/j.ica.2018.09.022
(c) H. Y. Qian, *Inorg. Nano-Met. Chem.* **2018**, *48*, 461–466; **DOI:**10.1080/24701556.2019.1569689
(d) H. Y. Qian, *Russ. J. Coord. Chem.* **2017**, *43*, 780–786. **DOI:**10.1134/S1070328417110070
2. (a) D. A. Megger, K. Rosowski, C. Radunsky, J. Kosters, B. Sitek, J. Muller, *Dalton Trans.* **2017**, *46*, 4759–4767; **DOI:**10.1039/C6DT04613D
(b) N. R. Palepu, J. R. Premkumar, A. K. Verma, K. Bhattacharjee, S. R. Joshi, S. Forbes, Y. Mozharivskyj, K. M. Rao, *Arabian J. Chem.* **2018**, *11*, 714–728. **DOI:**10.1016/j.arabjc.2015.10.011
3. (a) Y.-C. Liu, H.-L. Wang, S.-F. Tang, Z.-F. Chen, H. Liang, *Anticancer Res.* **2014**, *34*, 6034–6035;
(b) A. Erguc, M. D. Altintop, O. Atli, B. Sever, G. Iscan, G. Gormus, A. Ozdemir, *Lett. Drug Des. Discov.* **2018**, *15*, 193–202.
4. (a) M. Zhang, D.-M. Xian, H.-H. Li, J.-C. Zhang, Z.-L. You, *Aust. J. Chem.* **2012**, *65*, 343–350; **DOI:**10.1071/CH11424
(b) L. Shi, H.-M. Ge, S.-H. Tan, H.-Q. Li, Y.-C. Song, H.-L. Zhu, R.-X. Tan, *Eur. J. Med. Chem.* **2007**, *42*, 558–564. **DOI:**10.1016/j.ejmech.2006.11.010
5. N. P. Rai, V. K. Narayanaswamy, T. Govender, B. K. Manuprasad, S. Shashikanth, P. N. Arunachalam, *Eur. J. Med. Chem.* **2010**, *45*, 2677–2682. **DOI:**10.1016/j.ejmech.2010.02.021
6. (a) L.-H. Wang, X.-Y. Qiu, S.-J. Liu, *J. Coord. Chem.* **2019**, **DOI:**10.1080/00958972.2019.1590561
(b) X. W. Zhu, *Russ. J. Coord. Chem.* **2018**, *44*, 335–339; **DOI:**10.3103/S1068367418040213
(c) Z. H. Chohan, S. H. Sumrra, M. H. Youssoufi, T. B. Hadda, *Eur. J. Med. Chem.* **2010**, *45*, 2739–2747; **DOI:**10.1016/j.ejmech.2010.02.053
(d) O. Taheri, M. Behzad, A. Ghaffari, M. Kubicki, G. Dutkiewicz, A. Bezaatpour, H. Nazari, A. Khaleghian, A. Mohammadi, M. Salehi, *Transition Met. Chem.* **2014**, *39*, 253–259. **DOI:**10.1007/s11243-014-9798-9
7. D. Qu, F. Niu, X. Zhao, K.-X. Yan, Y.-T. Ye, J. Wang, M. Zhang, Z. You, *Bioorg. Med. Chem.* **2015**, *23*, 1944–1949. **DOI:**10.1016/j.bmc.2015.03.036
8. Bruker, SMART (Version 5.625) and SAINT (Version 6.01). Bruker AXS Inc., Madison, Wisconsin, USA, 2007.
9. G. M. Sheldrick, SADABS. Program for Empirical Absorption Correction of Area Detector, University of Göttingen, Germany, 1996.
10. G. M. Sheldrick, SHELXTL V5.1 Software Reference Manual, Bruker AXS, Inc., Madison, Wisconsin, USA, 1997.
11. J. Meletiadis, J. F. G. M. Meis, J. W. Mouton, J. P. Donnelly, P. E. Verweij, *J. Clin. Microbiol.* **2000**, *38*, 2949–2954.
12. A. Sarkar, S. Pal, *Polyhedron* **2007**, *26*, 1205-1210. **DOI:**10.1016/j.poly.2006.10.012
13. (a) D.-L. Peng, *Transit. Met. Chem.* **2016**, *41*, 843–848; **DOI:**10.1007/s11243-016-0086-8
(b) X. W. Zhu, *Russ. J. Coord. Chem.* **2018**, *44*, 421–424. **DOI:**10.1134/S1070328418070084
14. (a) D. L. Peng, *Russ. J. Coord. Chem.* **2017**, *43*, 404–410; **DOI:**10.1134/S1070328417060045
(b) Y. Li, L. Xu, M. Duan, J. Wu, Y. Wang, K. Dong, M. Han, Z. You, *Inorg. Chem. Commun.* **2019**, *105*, 212–216; **DOI:**10.1016/j.inoche.2019.05.011
(c) S. Guo, N. Sun, Y. Ding, A. Li, Y. Jiang, W. Zhai, Z. Li, D. Qu, Z. You, *Z. Anorg. Allg. Chem.* **2018**, *644*, 1172–1176; **DOI:**10.1002/zaac.201800060
(d) L.-Y. He, X.-Y. Qiu, J.-Y. Cheng, S.-H. Liu, S.-M. Wu, *Polyhedron* **2018**, *156*, 105–110; **DOI:**10.1016/j.poly.2018.09.017
(e) S.-J. Li, K. Li, X.-J. Yao, X.-Y. Qiu, *J. Coord. Chem.* **2015**, *68*, 2846–2857; **DOI:**10.1080/00958972.2015.1056171
(f) X.-Y. Qiu, *Chin. J. Inorg. Chem.* **2014**, *30*, 1667–1672;
(g) M. Liang, N. Sun, D.-H. Zou, *Acta Chim. Slov.* **2018**, *65*, 964–969; **DOI:**10.17344/acsi.2018.4625
(f) Z.-Q. Han, S. Han, Y. Wang, *Acta Chim. Slov.* **2016**, *63*, 200–203; (g) S.-S. Qian, X. Zhao, J. Wang, Z. You, *Acta Chim. Slov.* **2015**, *62*, 828–833.

Povzetek

Sintetizirali smo dva nova V^V kompleksa z bromo-substituiranima hidrazonoma, *N*'-(3-bromo-2-hidroksibenziliden)-3-hidroksi-4-metoksibenzohidrazidom (H_2L^1) in *N*'-(3-bromo-2-hidroksibenziliden)-3,5-dimetoksibenzohidrazidom (H_2L^2), $[VOL^1(OCH_3)(CH_3OH)]$ (**1**) in $[VOL^2(OCH_3)(CH_3OH)]$ (**2**) ter ju okarakterizirali z IR, UV-Vis in ^1H NMR spektroskopijo ter z monokristalno rentgensko analizo. V enojedrnih kompleksih je vanadijev atom oktaedrično koordiniran. Prostima hidrazonoma in kompleksoma smo določili antibakterijsko aktivnost na *S. aureus*, *B. subtilis*, *E. coli* in *P. fluorescence* ter antimikotično aktivnost na *C. albicans* in *A. niger*. Bromov atom na hidrazonskem ligandu lahko poveča antibakterijsko aktivnost.